Modelling Whole-Life Pavement Performance

Andrew Collop and David Cebon
Cambridge University Engineering Department, United Kingdom

ABSTRACT

A new 'whole-life' pavement performance model (WLPPM) has been developed that is capable of making deterministic pavement damage predictions due to realistic traffic and environmental loading. The WLPPM is divided into three central areas: (i) dynamic vehicle simulation, (ii) pavement primary response (stresses, strains etc.) simulation, and (iii) material damage (surface rutting and fatigue) simulation. Particular attention is given to modelling strength variations in the pavement and the pattern of dynamic tyre forces applied by a typical vehicle fleet.

The model is used to investigate the relationship between 'hot spots' (due to peak dynamic loads), 'weak spots' (due to initial pavement stiffness variations) and long-term pavement wear. It is concluded that both dynamic vehicle loads and asphalt layer stiffness variations can significantly influence long-term flexible pavement performance.

INTRODUCTION

A whole-life pavement performance model attempts to predict damage (rutting, fatigue cracking, roughness etc.) due to traffic and environmental loading conditions throughout the life of the pavement. A detailed review of previous whole-life pavement performance models that have included dynamic vehicle effects is given in [1] and will not be repeated in detail here. Typically, the whole-life models found in the literature [2-5] have been validated with measurements from the AASHO road test where the loading conditions were simplified by using one vehicle travelling at a constant speed to load each test lane. None of these models have investigated the relationship between damage propagation due to 'weak spots' in the pavement structure (produced by asphalt layer thickness variations etc.) and 'hot spots' on the pavement surface produced by peak dynamic loading. Consequently, there is some doubt as to which damage propagation mechanism is more important. This information is central to understanding the influence of dynamic loads on long-term flexible pavement wear.

The model described in this paper attempts to include the important mechanisms of pavement surface degradation using a deterministic (rather than statistical) approach. The first part of this paper briefly describes the operation of the Whole-Life Pavement Performance Model (WLPPM) using a simplified case study. The WLPPM is then used to evaluate the relative importance of dynamic loads and asphalt layer stiffness variations in three typical UK pavement constructions. For brevity, only the results from a minor road are presented.

WHOLE-LIFE PAVEMENT PERFORMANCE MODEL (WLPPM) DESCRIPTION

Figure 1 shows a schematic view of the WLPPM calculation procedure. It follows a similar pattern to the models developed by Ullidtz [4, 5] but differs considerably in the detail. The overall calculation procedure is summarised in the following few paragraphs and then described in detail.

Referring to figure 1, the initial inputs to the WLPPM are: (i) the specification of the pavement being simulated (i.e. layer thicknesses, mix specifications etc.), (ii) the time increment to be used in the simulation, (iii) the rate of traffic loading, and (iv) the climatic conditions the pavement is operating under. From this initial specification, a length of pavement surface profile is generated and divided into smaller sub-sections. Each sub-section is then assigned a random value for the thickness of the bound asphaltic layers, with the overall variation between sub-sections being representative of measured thickness variations. The thickness of the granular layer is assumed to be constant, and the subgrade is modelled as semi-infinite.

A time domain vehicle simulation is used to generate dynamic tyre forces for one or more vehicles that are a function of distance (or time) along the pavement. The vehicle model parameters and initial road surface roughness are chosen to best represent the traffic conditions for the type of pavement being simulated.

A set of primary response influence functions, for each sub-section and each mode of damage, is generated (i.e.

horizontal asphalt base strain for fatigue, subgrade strain and rate of permanent vertical surface deflection for rutting). These primary response influence functions are combined with the previously calculated dynamic tyre forces to give primary pavement response time histories at a large number of equally spaced points along the pavement.

These primary responses are combined with the appropriate pavement damage models (rutting and fatigue) and the number of load applications, to give damage as a function of distance along the pavement for the current time increment.

An updated surface profile is then generated by subtracting the calculated vertical deformation in the wheel path from the initial profile used for that time increment. This mechanism accounts for the effects of changing surface roughness on the dynamic tyre forces. The resulting fatigue damage is used to reduce the elastic modulus of the asphaltic material for each sub-section. This mechanism reflects the effects of cumulative fatigue damage on the primary responses and hence subsequent pavement damage.

The above process is then repeated for the next time increment, and so on, until the pavement has reached the end of its serviceable life. The following section describes the models used in each area of the WLPPM in more detail.

CLIMATIC FACTORS

Many climatic and environmental factors influence the performance of a flexible pavement. The only environmental effects that are currently included in the WLPPM are the temperature and ageing of the asphalt layer. However, due to the modular structure of the program, it is relatively simple to include other environmental effects such as the effects of frost and moisture on unbound materials, (e.g. [6, 7]) provided these effects can be easily quantified.

Temperature of the Asphalt Layer Changes in the temperature of the asphalt layer affect the elastic and viscous properties of the bitumen. The variation in the monthly mean air temperature T_{air} (°C) was assumed to be sinusoidal of the form:

$$T_{air} = \frac{\left(T_{air}^{max} + T_{air}^{min}\right)}{2} + \frac{\left(T_{air}^{max} - T_{air}^{min}\right)}{2} \cos\left(\frac{(U - U_0)\pi}{6}\right), \quad (1)$$

where T_{air}^{max} is the maximum monthly air temperature throughout the year (°C), T_{air}^{min} is the minimum monthly air temperature throughout the year (°C), U is the month number from the new year and U_0 is the month number corresponding to the maximum monthly temperature.

Ullidtz [4] noted that, in many cases, EQ(1) gave a good approximation to measured mean monthly temperatures. If more detailed temperature data is available, it can easily be incorporated in the WLPPM. For simulation time increments of longer than 1 month, the air temperature was determined by averaging the appropriate monthly temperatures together (determined from EQ(1)).

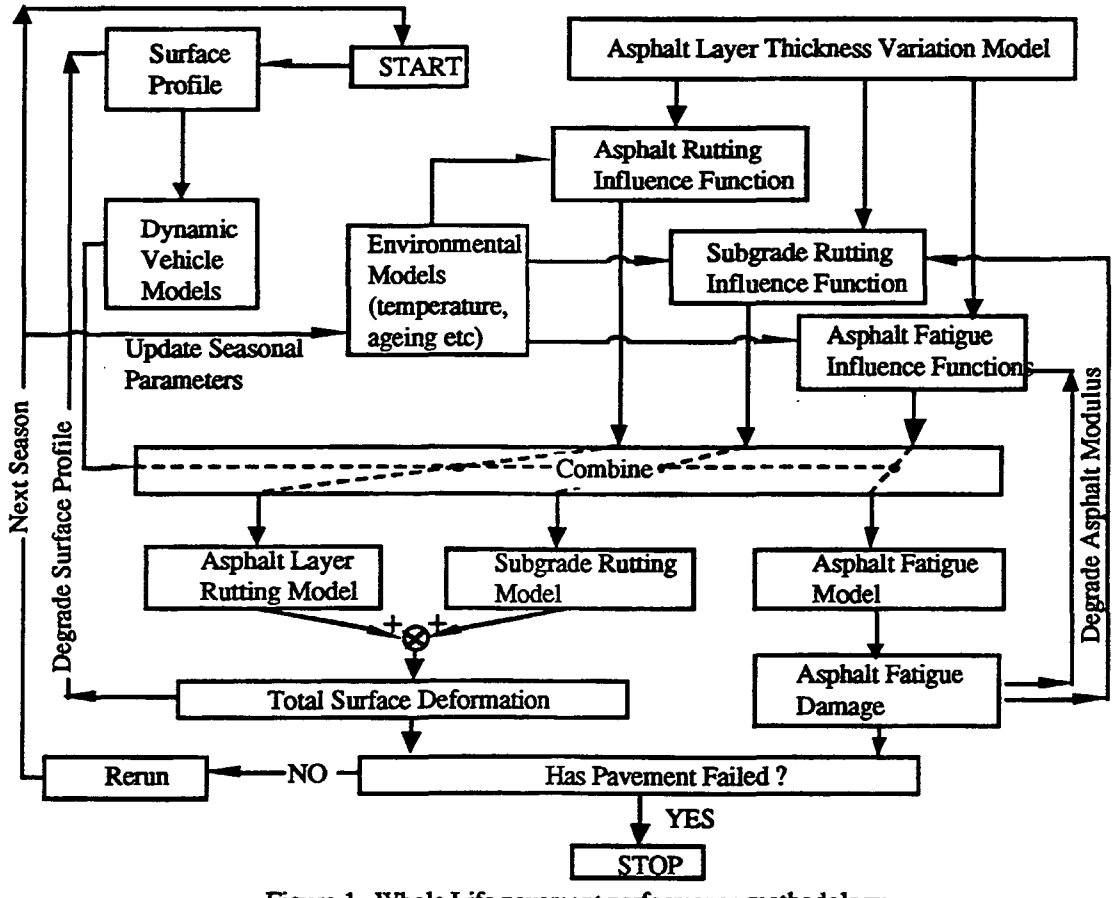

Figure 1. Whole Life pavement performance methodology.

Predicting the temperature profile of the asphaltic material (T_{asp}) from the air temperature (T_{air}) is complicated, and requires detailed information about the thermal properties of the asphalt and the ambient conditions (see, for example [8]). Consequently, a simplified approach was used, where the effective monthly temperature of the asphalt layer was estimated from the air temperature using the following empirical equation (see [9] for further details):

$$T_{asp} = T_{air}\left(1+\frac{76.2}{h_{asp}+304.8}\right)-\frac{84.7}{h_{asp}+304.8}+3.3, \quad (2)$$

where (T_{asp}) is the effective surface layer temperature (°C), (T_{air}) is the measured mean air temperature (°C), and h_{asp} is the thickness of the surface layer (mm).

PAVEMENT SURFACE DISPLACEMENT PROFILE MODEL

The pavement surface roughness profiles were generated from the equations given in reference [10] for single sided pavement surface profile spectral densities $S_Z(\gamma)$:

$$S_Z(\gamma) = c\gamma^{-w} \qquad (0<\gamma<\gamma_{max}), \quad (3)$$

where γ is the wavenumber (cycles/m), $w=2.5$ and c as follows:

Class	Typical range of $c/10^{-8}$ m$^{1/2}$cycle$^{3/2}$	Geom. mean value of $c/10^{-8}$ m$^{1/2}$cycle$^{3/2}$
Motorway	3–50	12.2
Principal	3–800	49.0
Minor	50–3000	387.3

A one-dimensional surface displacement history was generated from EQ(3) by applying a set of random phase angles, uniformly distributed between 0 and 2π, to a series of coefficients derived from the desired spectral density (see [11] for further details) and applying the inverse Fast Fourier Transform (FFT). Typically, the resulting surface displacement profiles were generated with data points every 0.1m giving a lower wavelength limit (corresponding to the Nyquist frequency) of 0.2m. The upper wavelength limit $(1/\gamma_{max})$ was several hundred metres.

In order to quantify pavement surface roughness using a single statistic is used in this paper: the International Roughness Index (IRI) [12]. The IRI is the ratio of the accumulated suspension motion divided by the total distance travelled, calculated from the response of a linear 'quarter car' vehicle model travelling at 80km/h over the pavement profile of interest. On the IRI scale, a perfectly smooth pavement is rated as 0, an asphalt pavement in good condition is rated at approximately 2mm/m and a severely damaged pavement may be rated as high 10mm/m. A detailed description of the method used to calculate the IRI for a given profile is given in reference [12].

DYNAMIC VEHICLE SIMULATION

The subject of dynamic tyre force modelling was extensively reviewed by Cole in 1990 [13] and will not be repeated in detail here. Cole and Cebon [14] developed various non-linear two and three dimensional vehicle models which they validated with experimental measurements performed on the TRL test track. They concluded from their research that a two dimensional vehicle model should be satisfactory for predicting the tyre forces of typical leaf sprung articulated vehicles with well damped unsprung mass modes of vibration, operating under typical UK conditions of speed and road roughness. However, Cebon [15] noted that a simpler linear 'quarter car' vehicle model has dynamic characteristics that are broadly representative of the majority of single axle truck suspensions in current use. Consequently, a linear 'quarter car' vehicle model was used in the case studies described in this paper. The WLPPM can incorporate more realistic (validated) articulated vehicle models without difficulty, but at the expense of significantly increased computation time. 'Quarter car' parameters for a fully laden vehicle with typical air and steel suspensions (from reference [16]) are shown in figure 2.

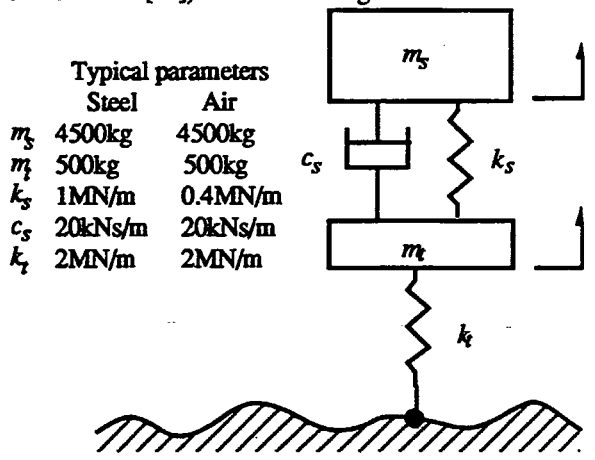

Figure 2. 'Quarter Car' vehicle model.

The dynamic tyre forces generated by the vehicle model were obtained by numerically integrating the equations of motion using the pavement surface profile displacement as the input to the tyre (see [13] for further details). If the pavement surface profile is sufficiently rough, the model incorporates a facility for the wheel to leave the ground.

PAVEMENT PRIMARY RESPONSE MODEL

Previous work on pavement primary response models was extensively reviewed by Hardy in 1990 [17] and Cebon in 1993 [15] and will not be repeated here. Hardy and Cebon [18] concluded that the influence function method is sufficiently accurate to calculate the dynamic response of a pavement to dynamic tyre forces, providing the pavement model includes the effect of speed accurately. Consequently, a modified version of the VESYS IIIA quasi-static pavement model [19] (modifications by Cebon for NCHRP project 1-25, see [20]) was used to generate the required primary pavement response influence functions. Typical contact radii for single and super single tyres were taken to be 108mm and 135mm respectively [21]. Dual tyres were modelled as two separate circular contact areas of radius 108mm.

All the pavement structures investigated were modelled as three layer systems comprising; (i) an asphaltic layer (wearing course plus base course), (ii) a granular sub-base layer, and (iii) a subgrade or soil layer. The primary

response model required the elastic properties (Young's modulus and Poisson's ratio) and the thickness of each layer (except the subgrade which is of infinite thickness). The methods used to obtain these parameters are described in the following sub-sections.

Asphalt Surface Layer Elastic Properties Typically, a full-depth asphaltic pavement consists of three separate layers of bituminous material; a wearing course, a road base and a basecourse. The properties of the road base and basecourse are usually similar whereas the wearing course has different mix proportions and hence properties. However, according to Brown [22], typical UK wearing courses have a relatively small influence on the structural performance of the pavement and it may be combined with the other two layers. Consequently, a single asphaltic layer of typical road base (or basecourse) material has been used to represent the asphaltic layers of a full-depth flexible pavement.

The elastic modulus of the bituminous binder E_b(MPa) was calculated using the following equation derived from the Van der Poel nomograph [23]:

$$E_b = 1.157\times10^{-7}\, t_l^{-0.368}\, 2.718^{-PI^{(R)}}\left(T_{RB}^{(R)} - T_{asp}\right)^5, \quad (4)$$

where $T_{RB}^{(R)}$ is the recovered bitumen 'Ring and Ball' softening temperature $(°C)$, T_{asp} is the temperature of the asphalt layer $(°C)$, $PI^{(R)}$ is the recovered bitumen 'Penetration Index' and t_l is the loading time (secs).

The bitumen properties recovered after the asphalt has been mixed and laid $\left(T_{RB}^{(R)}\right.$ and $\left.PI^{(R)}\right)$ were obtained from the initial penetration of the bitumen $P^{(I)}$ using the following empirical equations [22]:

$$P^{(R)} = 0.65P^{(I)}, \quad (5a)$$

$$T_{RB}^{(R)} = 98.4 - 26.35\log_{10}\left(P^{(R)}\right), \quad (5b)$$

$$PI^{(R)} = \frac{27\log_{10}P^{(I)} - 21.65}{76.35\log_{10}P^{(I)} - 232.82}, \quad (5c)$$

where $P^{(I)}$ is the initial penetration of the bitumen.

The effective loading time t_l was estimated from [23, 24]:

$$\log_{10}(t_l) = 5\times10^{-4}\, h_{asp} - 0.2 - 0.94\log_{10}(V), \quad (6)$$

where h_{asp} is the thickness of the asphalt layer (mm) and V is the vehicle speed (km/hr).

The elastic modulus of the asphalt mixture E_m(MPa) was calculated using the following empirical equation [22]:

$$E_m = E_b\left[1 + \frac{257.5 - 2.5VMA}{n(VMA-3)}\right]^n, \quad (7)$$

where $n = 0.83\log_{10}\left(\frac{4\times10^4}{E_b(\text{MPa})}\right)$ and

VMA = % Voids in Mixed Aggregate

= % vol. air voids + % vol. bitumen.

The thickness of the asphaltic material was determined from the standard UK design procedure for the type of pavement being simulated (see [25] for further details).

Poisson's ratio for asphaltic material has been shown to be highly dependent on temperature with values ranging from 0.15 (low temperatures) to 0.45 (high temperatures) [26]. A typical constant value was taken to be $\upsilon_{asp} = 0.4$ [22].

Ageing of the Asphalt Layer Ageing of bituminous materials has been shown to occur in two stages: (i) short term and (ii) long term [27-29]. Short term ageing occurs during manufacture and laying, and is mainly due to the loss of volatile components and oxidation while the mix is hot. Long term ageing is mainly due to progressive oxidation of the mixture while it is in service.

Short term ageing was included in the model by using typical bitumen properties recovered after mixing and laying $\left(T_{RB}^{(R)}, PI^{(R)}, \text{etc.}\right)$.

Long term ageing of the bitumen was accounted for by increasing the recovered 'Ring and Ball' softening point temperature $T_{RB}^{(R)}$, with the age of the pavement, according to a one-dimensional kinetic diffusion model developed by Verhasselt and Choquet [29]:

$$T_{RB}^{(R)}\Big|_{t=t_1} = T_{RB}^{(R)}\Big|_{t=0} + \sqrt{A\,t}, \quad (8)$$

where $T_{RB}^{(R)}$ is the recovered 'Ring and Ball' temperature $(°C)$ at time $t = t_1$, $T_{RB}^{(R)}\Big|_{t=0}$ is the initial Ring and Ball temperature $(°C)$ at time $t = 0$, A is the reaction constant $(°C^2/\text{hour})$ and t is the time (hours).

Verhasselt and Choquet [29] determined the value of A from accelerated laboratory ageing tests on different types of bitumen and they found that the reaction constant A depended strongly on the temperature of the bitumen. Consequently, to apply EQ(8) to an in-service pavement where the temperature of the asphalt layer is constantly changing, they related the mean annual air temperature to the effective temperature at which the reaction constant should be determined (see [29] for further details). For typical climatic conditions in Belgium, the average reaction constant A was found to vary between 1.2×10^{-3} to 2.1×10^{-3} $°C^2$/hour depending on the type of bitumen being considered. Verhasselt and Choquet used these values of the reaction constant to predict ageing of the whole asphalt layer for typical pavements in Belgium. They obtained a reasonable agreement with the measured ageing of the material. A value of $A = 1.65\times10^{-3}$ $°C^2$/hour together with EQ(8) was therefore used to model ageing of the whole asphalt layer in a typical UK pavement.

An ageing model of this type will affect both the elastic and viscous properties of the asphaltic material since they both depend on the properties of the bituminous binder.

Subgrade Layer Elastic Properties The elastic modulus of the subgrade E_{sub}(MPa) was estimated from the empirical equation [22]:

$$E_{sub} = 10CBR, \quad (9)$$

where CBR is the 'California Bearing Ratio' of the subgrade.

For details of the CBR test refer to [30]. Poisson's ratio for soil has been shown to depend on the degree of soil cohesion and ranges from 0.3 (cohesive-less soils) to 0.5 (very plastic clays, cohesive soils) [26]. A typical value was taken to be $\upsilon_{sub} = 0.4$ [22].

Granular Sub-Base Layer Elastic Properties The elastic modulus of the granular base layer was taken to

be a constant 100MPa $\left(\text{i.e. } E_{gra} = 100\,\text{MPa}\right)$ corresponding to a good quality granular base [22]. The thickness of the granular base was taken to be a standard 200mm from [22].

Poisson's ratio for the granular material depends on the degree of crushing of the material and ranges from 0.3 (crushed material) to 0.4 (unprocessed gravels/sands) [26]. A typical value was taken to be $\upsilon_{gra} = 0.3$ [22].

FATIGUE CRACKING MODEL

From [31] it was concluded that under almost all circumstances, traffic-generated fatigue damage initiates at the base of the bound asphaltic layers and propagate towards the surface. Thermal load cycles and stress concentrations at the surface due to non-uniform contact conditions have little effect. Consequently, the fatigue model chosen for the WLPPM was a 'traditional' fatigue model which assumes that cracks originate at the bottom of the asphaltic layers, where the tensile strain is greatest, and propagate vertically upwards towards the pavement surface.

Simplified laboratory test on asphaltic specimens have led to a relationship between fatigue life and strain of the form (see, for example [15, 32, 33]):

$$N_f^{(i)} = k_1\,\varepsilon_i^{-k_2}, \tag{10}$$

where $N_f^{(i)}$ is the number of cycles to failure at strain level ε_i (micro strain), and k_1 and k_2 are fatigue constants describing the fatigue behaviour of the material.

Cooper and Pell [34] examined the effect of various asphalt mix variables and temperature on the fatigue life of over 2000 specimens of a wide variety of both basecourse and wearing course asphaltic mixes. They concluded that fatigue performance, on the basis of applied tensile strain, was primarily influenced by the type and amount of bituminous binder. The effects of temperature and loading time were assumed to be accounted for by their effect on elastic stiffness. However, it was found that the resulting fatigue law gave conservative results when compared with experimental field data and thus required 'calibrating' [35]. This calibration was performed for average UK conditions giving fatigue constants k_1 and k_2 as a function of the properties of the asphalt mix [35]:

$$\begin{aligned} \log_{10}(k_1) &= 14.39\log_{10}(V_B) + 24.2\log_{10}\left(T_{RB}^{(I)}\right) - 46.06, \\ k_2 &= 5.13\log_{10}(V_B) + 8.63\log_{10}\left(T_{RB}^{(I)}\right) - 15.8, \end{aligned} \tag{11}$$

where V_B is the percentage volume of bituminous binder and $T_{RB}^{(I)}$ is the initial 'Ring and Ball' softening temperature of the bitumen $\left(^{\circ}\text{C}\right)$.

The initial 'Ring and Ball' softening temperature $T_{RB}^{(I)}$ of the bitumen may be obtained from EQ(5b) by replacing the recovered penetration $P^{(R)}$ with the initial penetration $P^{(I)}$. The fatigue properties defined by EQ(11) include a factor of 440 to allow for differences between laboratory test conditions and those in the pavement [35]. This 'correction' comprises a factor of 20 for rest periods between load applications, a factor of 20 for the time taken for the crack to propagate through the bituminous layer, and a factor of 1.1 for the lateral distribution of wheel loads on the pavement surface [35].

The accumulation of fatigue damage D at each point along the road due to the passage of a vehicle was estimated using Miner's hypothesis of linear damage accumulation [24]:

$$D = \sum_{i=1}^{j} \frac{N^{(i)}}{N_f^{(i)}} \tag{12}$$

where $N^{(i)}$ is the number of cycles of strain level ε_i, $N_f^{(i)}$ is the number of cycles to failure of strain level ε_i and j is the number of different strain levels.

Gillespie *et al.* [20] investigated two different methods for reducing a complex strain time history to a number of equivalent strain cycles, 'rainflow' counting and 'peak' counting. The 'rainflow' counting method involves determining the overall strain range (largest peak to lowest valley) and removing this from the history. This is taken as the first strain cycle and the process is repeated until all strain reversals have been considered. This method is commonly used for metal fatigue due to complex time histories and corresponds to counting complete hysteresis loops in the stress-strain curve for the material (see [20] for further details). The 'peak' counting method considers just the peak tensile strain to be the equivalent strain cycle. This type of approach cannot account for compressive strains between tensile peaks or strain levels that do not recover to zero between multiple axles. Gillespie *et al.* [20] concluded that the ranking of the vehicles in their study was not greatly affected by the method of cycle counting. Consequently, the simpler 'peak' counting method was used in the WLPPM.

PERMANENT DEFORMATION MODEL

The rutting model used in the WLPPM comprised two parts. The first part is the linear visco-elastic rutting model presented in [36], which was used to model the asphaltic layers of the pavement where permanent deformation is primarily due to viscous flow. This linear visco-elastic calculation requires the viscosity of the bituminous binder, and the mix specification. The viscosity of the bituminous binder λ_b (MPa.s) was obtained using the following approximate expression [4]:

$$\lambda_b = 3\times10^{-6}\left\{1.3\times10^{\left[3+\left(T_{RB}^{(R)}-T_{asp}\right)/10\right]}\right\}. \tag{13}$$

The effective viscosity of the asphalt mix was then obtained from the following equations (see [36] for more details):

$$\log_{10}(\lambda_a) = \Phi_1(VMA) + \Phi_2(VMA)\log_{10}(\lambda_b), \tag{14}$$

where λ_a is the extensional viscosity of the asphalt mix (MPa.s), λ_b is the extensional viscosity of the bitumen (MPa.s) at the temperature of the mixture, and

$\Phi_1(VMA) = 1.86\times10^{-3}\,VMA^2 - 1.65\times10^{-1}\,VMA + 6.98$

$\Phi_2(VMA) = -2.2\times10^{-4}\,VMA + 7.5\times10^{-1}$.

A simple relationship between vertical subgrade strain and permanent deformation was used to include rutting in the subgrade and granular layer. This relationship is of the same general form as the model used to relate vertical subgrade strain to permanent surface deflection (see, for example [37, 38]). The incremental permanent deformation in the

subgrade and granular layer due to a single axle load may be expressed as:

$$\delta_i = L_1 \varepsilon_i^{L_2}, \qquad (15)$$

where δ_i is the incremental vertical permanent deformation in the subgrade and granular layer due to vertical subgrade compressive strain ε_i, and L_1 and L_2 are material constants.

This model will be referred to as the subgrade rutting model. As with the fatigue model, Miner's cumulative damage law, EQ(12), and peak cycle counting were used to calculate subgrade rutting due to strain cycles of different magnitudes.

In the literature reviewed by Hardy [17], the value of the exponent L_2 in the damage law relating vertical subgrade strain to permanent surface deformation was found to vary considerably from 1.85 to 7.14 depending on the pavement design and the test conditions. Brown [38] investigated the relationship between the maximum allowable elastic subgrade strain and the number of load repetitions and concluded that a value of $L_2 = 3.57$ was suitable for typical UK pavements. However, no models capable of predicting these constants from the subgrade specification and operating conditions were found in the literature. The parameter L_2 was therefore considered to be an unknown input variable to the WLPPM and its importance was investigated in a parametric study.

The multiplicative subgrade rutting constant L_1 in EQ(15) directly affects the proportions of surface rutting to subgrade and granular layer rutting. These proportions have been shown to vary from pavement to pavement. In a typical UK pavement, approximately half the rutting was found to occur in the surfacing and roadbase and half in the sub-base and subgrade [38, 39]. Consequently, the subgrade rutting multiplicative constant L_1 in EQ(15) was chosen such that, for a thick asphalt pavement (250mm), at a mean yearly air temperature of 10°C (typical of a UK climate [35]), approximately half the rutting occurred in the asphaltic layers and half in the subgrade and granular layers.

ASPHALT MODULUS DEGRADATION MODEL

Several studies on experimental and in-service pavements have shown that there is a significant relationship between long-term pavement performance and changes in the transient deflection of the pavement surface (see, for example [40-42]). To include this effect in the WLPPM, a modulus degradation model has been developed.

Surface deflection data was obtained from two Accelerated Loading Facility (ALF) trials [43, 44] performed by the Australian Road Research Board (ARRB). A back calculation procedure (with appropriate temperature correction [45]) was used to determine the set of layer moduli that gave the best fit between calculated and measured surface deflection bowls. The moduli were plotted as a function of the cumulative fatigue damage experienced by the test section using EQ(12). The resulting asphalt modulus degradation model was of the following form:

$$\begin{aligned} E/E_0 &= \exp^{KD} && D < 1, \\ E/E_0 &= (E/E_0)_c && D \geq 1, \\ K &= \log_e (E/E_0)_c . \end{aligned} \qquad (16)$$

where E/E_0 is the reduction in elastic modulus of the asphaltic material, D is the cumulative fatigue damage (see EQ(12)) and $(E/E_0)_c$ is a constant that determines the level of modulus reduction corresponding to the end of the fatigue life of the asphalt (i.e. $D = 1$).

Figure 3 shows a typical plot of EQ(16), with $(E/E_0)_c = 0.2$, together with the back calculated data, using measured surface deflections from the ALF trials. It can be seen that the moduli conform reasonably well to the modulus degradation law. A detailed description of the back calculation method is given in reference [45].

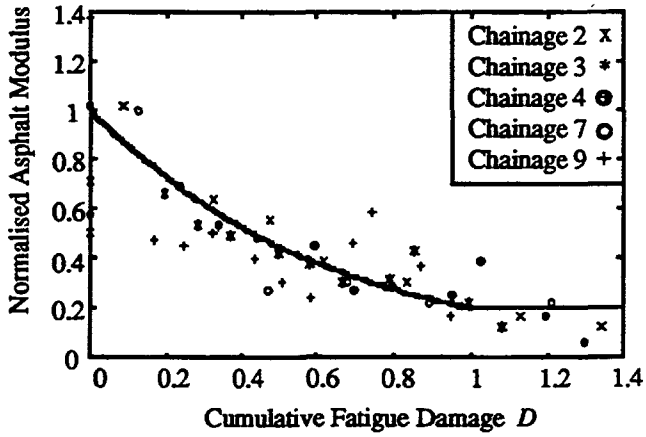

Figure 3. Reduction in normalised asphalt layer modulus.

PAVEMENT STIFFNESS VARIATIONS

One of the major causes of stiffness variations along the length of the pavement is variations in the thickness of the asphalt layer. The method used to quantify this variation is explained in this section.

Figure 4 shows the thickness spectrum S_h calculated using a number of sections of measured data from the A500T trunk road. The data was measured by GB Geotechnics using ground penetrating radar techniques (e.g. [46, 47]). Also plotted in figure 4 is a fitted equation of the form:

$$S_h(\gamma) = \frac{F}{1 + (\gamma/\gamma_0)^H}. \qquad (17)$$

The fitted constants were found to be; $F = 6.3 \times 10^{-2}$ m^3/cycle, $\gamma_0 = (3.13 \times 10^3)^{2.25}$ m/cycle and $H = 2.25$. It can be seen by comparing EQ(17) with EQ(3) (the equation for the spectral density of the pavement profile surface displacement) that the value of the exponent is similar (2.25 from EQ(17), compared with 2.5 from EQ(3)). Consequently, the amplitude of the thickness spectrum and the amplitude of the surface displacement spectrum decrease at approximately the same rate with increasing wavenumber (decreasing wavelength).

A random asphalt layer thickness displacement history can be obtained from EQ(17) using the same inverse FTT method used to obtain the pavement surface profile. Note that this method gives a Gaussian amplitude distribution, which agrees well with the measurements. The phase relationship between the various roughness components in the surface profile and the thickness profile is not known. This relationship would require information about the cross-

spectrum between the surface roughness and the thickness. Such information could only be obtained from simultaneous measurements of the surface profile and thickness, and data of this type could not be found. Consequently, in the absence of suitable cross-spectral information, the thickness profile was assumed to be uncorrelated with the surface profile. This was implemented by using random phase angles to generate the thickness profile that were uncorrelated with the random phase angles used to generate the surface profile. Any other degree of correlation could be included in the model, if suitable cross-spectral information was available, using the method in [11].

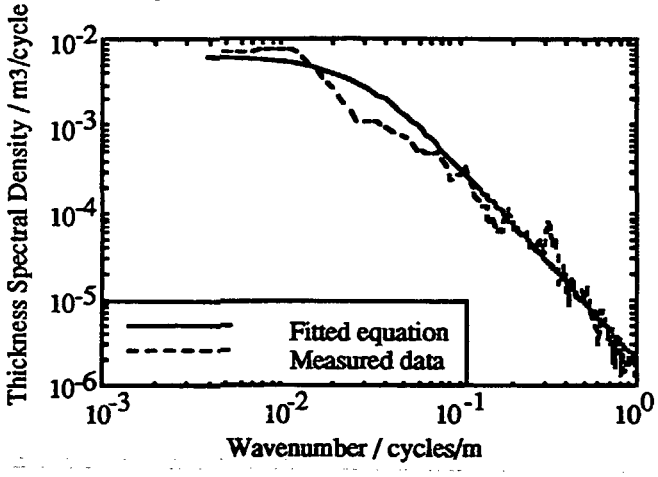

Figure 4. Asphalt layer thickness spectral density.

To determine thickness profiles for pavements with a different mean asphalt layer thickness to the A500T (different mean asphalt layer thickness), the thickness spectrum (EQ(17)), was scaled such that ratio of the standard deviation to the mean asphalt thickness was the same for all pavements.

Once a thickness profile was generated, it was divided into a number of equally spaced, discrete sub-sections where the thickness was assumed constant. This simplified thickness variation was then used in the WLPPM.

To avoid step changes in the primary responses at a boundary between sub-sections with different asphalt layer thicknesses and/or different asphalt layer moduli, linear interpolation was used between the two adjoining influence functions (see [45] for further details).

SIMPLIFIED CASE STUDY

To illustrate the various features of the WLPPM described above, a simplified case study is examined here. The vehicle loading was applied using a linear 'quarter car' vehicle model travelling at a constant speed of 22.5m/s (80km/h) over a 100m length of surface profile. The loads generated by the vehicle model were applied to the pavement through a 'super-single' tyre with a contact patch radius of 0.135m. The parameters used in the 'quarter car' model corresponded to a fully laden vehicle with a steel spring suspension.

A typical 50 pen modified hot rolled asphalt was used, and to simplify the simulations, all the material properties that are functions of temperature (e.g. asphalt modulus, viscosity etc.) were fixed at a temperature of 10°C. Full details of the mix specification and input parameters are given in the Appendix. For each of the case studies, the nominal thickness of the asphalt layer was 250mm and ageing of the asphaltic material was assumed not to occur. The subgrade was assumed to have a *CBR* of 4%. Where a random surface profile was required, an initial profile with IRI = 2 was used. This corresponds to the typical roughness of a new principal road.

To include asphalt layer thickness variations in the model the pavement was divided into 0.5m sub-sections, each of constant thickness. To limit the number of computations required, the random thickness variation was discretised into 6 levels and the modulus of the asphalt layer was degraded in 10% steps (9 increments altogether). The pavement surface profiles were updated 80 times (approximately every 260,000 load passes). It was found that, using the above parameters, a satisfactory trade off was achieved between computation speed and convergence of the results (see [45] for further details).

The rutting due to the static vehicle loads at the end of the loading period (i.e. after 20.75 million load applications) was approximately 20mm. This is typically taken to be the point at which a flexible pavement has failed [22].

To investigate the importance of the subgrade rutting law, the rutting exponent L_2 in EQ(15) was taken to be either 1 or 4. The corresponding values of the multiplicative rutting constant L_1, were chosen such that approximately half the rutting occurred in the surface and half in the lower layers: $L_1 = 2.47 \times 10^{-3}$ mm and $L_1 = 3.31 \times 10^{8}$ mm respectively. The importance of the modulus degradation law feedback loop on the primary response model was also investigated.

RANDOM THICKNESS VARIATION AND A FLAT PROFILE

This case study examines damage propagation on a pavement with a random asphalt layer thickness variation and an initially flat surface profile. The random thickness variation was created using the procedure detailed earlier. Figure 5 shows the random asphalt layer thickness distribution (dashed line) together with the distribution averaged over 0.5m intervals and discretised into 6 levels (dashed line). This discretised distribution was used in the WLPPM.

Figure 6 shows the initial pavement surface profile together with profiles after 10.11 million and 20.75 million load passes using $L_2 = 1$ in the subgrade rutting law (EQ(15)). It can be seen from this figure that the surface level drops as the number of load passes increases. This corresponds to the formation of a rut in the wheelpath. For no modulus degradation (solid line), the pavement surface profile degrades at an approximately uniform rate due to the static vehicle loads, with only a small effect from dynamic loading induced by the surface roughness. Also shown in this figure (dashed line) are the results of the same case, but including degradation of the asphalt layer modulus as the pavement becomes progressively fatigue damaged. It can be seen that in this case, including this feedback loop has

virtually no effect on the surface profile. This is because, even at the most heavily loaded areas, only a small proportion of the fatigue life has been used up by the time the permanent deformation becomes excessive.

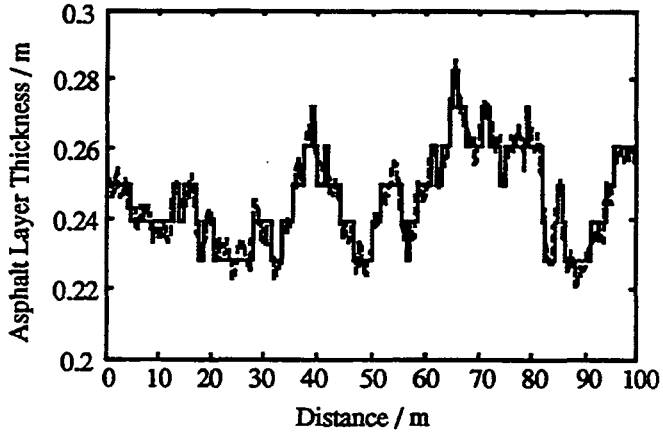

Figure 5. Random asphalt layer thickness variation.

Figure 7 shows the corresponding situation using $L_2 = 4$ in the subgrade rutting law (EQ(15)). It can be seen from this figure that, with no modulus degradation (solid line), the magnitude of the damage is significantly increased and dynamic loads induced by the initial asphalt layer thickness profile have a more prominent effect. For example, it can be seen that although the average rutting (due to the static loads) after 20.75 million load passes is 20mm, the profile at 90m along the pavement shows a depression approximately 4m long and 40mm deep (20mm below the 'static' rut depth). It can also be seen by comparing this figure with the input thickness profile (figure 5) that the depression has formed where the asphalt layer is at its thinnest.

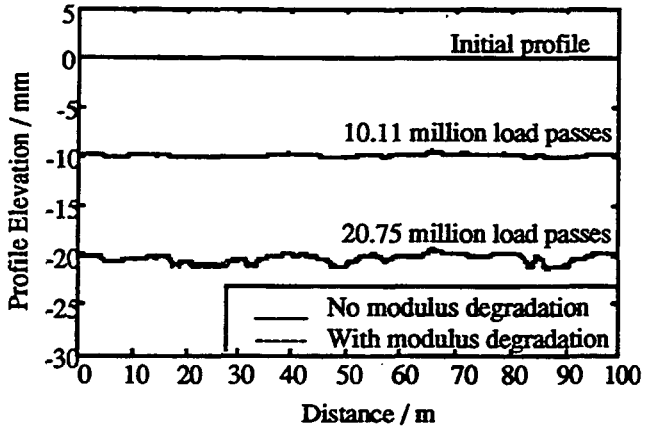

Figure 6. Pavement surface displacement profiles at various loading stages, using $L_2 = 1$.

It can also be seen from this figure that the surface irregularities excite the modes of vibration of the vehicle model with the result that the downstream surface profile fluctuates about a mean rut depth. The wavelength of these fluctuations corresponds to the frequency of sprung mass vibration of the vehicle model (approximately 2.5Hz). The dashed line in figure 7 show the same test case but including degradation of the asphalt layer modulus. It can be seen that including this damage feedback mechanism increases the amount of permanent deformation, particularly at the most heavily loaded areas (troughs). This is because the cumulative fatigue damage, and hence modulus reduction, is greatest at these areas of greatest load concentration and this effect becomes more important when the subgrade is more sensitive ($L_2 = 4$). Consequently, the permanent vertical subgrade strain is increased at these locations, resulting in an increased rate of subgrade deformation (rutting).

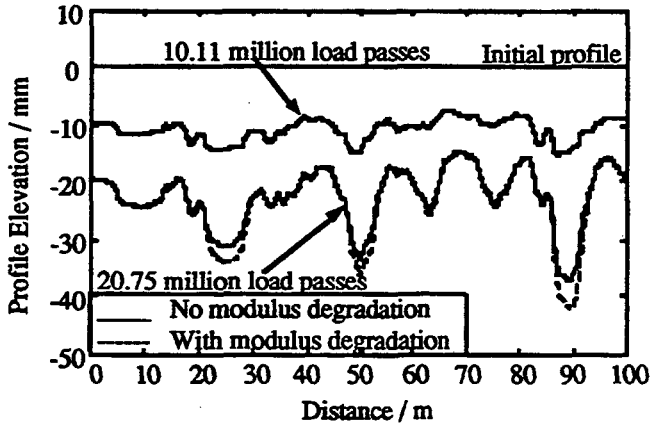

Figure 7. Pavement surface displacement profiles at various loading stages, using $L_2 = 4$.

PARAMETER STUDY

The case study examined in the previous section was useful to help explain the various component parts of the WLPPM. However, it is not representative of in-service conditions. The following section explains the method used to simulate a realistic fleet of heavy goods vehicles operating on a number of typical UK pavement constructions. For brevity, only the results for the minor road are presented.

SPATIAL REPEATABILITY

To assess the importance of dynamic tyre forces in the pavement degradation process, it is important that the dynamic loads used in the WLPPM are representative of the distribution of loads applied to the pavement by a typical vehicle fleet. In particular, the levels of 'spatial repeatability' of dynamic loads should be included accurately [49].

In the WLPPM, four quarter car simulations were used to represent measured vehicle fleet speed variations (taken from the National Speed Survey [48]). The values of suspension stiffness for each model was chosen such that the overall pattern of loading applied to the pavement by the simulated vehicle fleet (spatial repeatability) matched previously measured patterns of loading from the A34 in Oxfordshire [45, 49, 50]. Further details of this process are given in [45] and details of the suspension stiffnesses and speed ranges are given in the Appendix.

WLPPM INPUT PARAMETERS

The thickness of the asphalt layer was taken to be 125mm (from standard UK design procedure [25]) and the length of the pavement section simulated was 100m. As in

the simplified case study, a typical 50 pen modified hot rolled asphalt was used for the bituminous binder and the subgrade was assumed to have a *CBR* of 4%. Full details of the mix specification and input parameters are given in the Appendix. An initial IRI roughness of 3 was used. The variation in monthly air temperature for each pavement type was sinusoidal, with a mean temperature of 11°C and a temperature amplitude of 7°C. These are typical of UK climatic conditions [38].

One of the conclusions from the simplified case study is that predictions of damage are significantly influenced by the exponent chosen in the subgrade rutting model (EQ(15)). For this study two different assumptions were considered. In the first, a value of $L_2 = 3.5$ was used. This corresponds to the value proposed by Brown [38] for use with pavement design procedures in the UK. The value of the subgrade multiplicative constant was taken to be $L_1 = 4.63 \times 10^6$ mm, giving approximately half the rutting in the asphaltic material and half the rutting in the lower layers for a thick pavement with an air temperature of 10 °C. For the second assumption a value of $L_2 = 1$ was used. This can be considered to be a pessimistic estimate of subgrade damage and gives lower layer rutting that is proportional to the instantaneous value of the vertical subgrade strain. The value of the subgrade multiplicative constant was taken to be $L_1 = 2.47 \times 10^{-3}$ mm, giving approximately half the rutting in the asphaltic material and half the rutting in the lower layers for a thick pavement with an air temperature of 10 °C.

To assess the importance of various factors, 4 cases were considered:

Case	Initial Profile	Thickness	Vehicle Loads
0	Smooth	Uniform	Static
1	Random	Uniform	Dynamic
2	Smooth	Random	Static
3	Random	Random	Dynamic

To compare results from the 4 cases, two criteria were used. The first is denoted the 'Pavement Life Reduction Factor' (PLRF). For case i, this is defined as:

$$\text{PLRF}^{(i)} = \frac{N^{(0)} - N^{(i)}}{N^{(0)}} \times 100\%, \qquad (i = 1,2,3), \quad (18)$$

where $N^{(i)}$ is the number of load passes in case i required to produce 'critical' conditions, and $N^{(0)}$ is the number of load passes in case 0 required to produce 'critical' conditions.

'Critical' conditions are defined to be the first point where the 95th percentile rut depth reaches 10mm (often defined as the point where overlaying is required [25]) or the 95th percentile fatigue damage reaches 0.5. The 95th percentile level can be interpreted as the damage incurred at the worst 5% of locations along the pavement. The PLRF is a measure of the importance of dynamic loads or asphalt layer thickness variations on predicted pavement life.

The second criterion is the 'Simulation Error' (SE). For case i, this is defined as:

$$\text{SE}^{(i)} = \frac{F^{(3)} - F^{(i)}}{F^{(3)}} \times 100\%, \qquad (i = 0,1,2), \quad (19)$$

where $F^{(i)}$ is the case i 'failure' condition when the case 3 'failure' condition $F^{(3)}$ is reached.

'Failure' conditions are defined to be the point where the 95th percentile rut depth reaches 20mm or the 95th percentile fatigue damage reaches 1.0. The SE is a measure of the error in predicted pavement damage if dynamic loads and/or asphalt layer thickness variations are neglected.

'Failure' conditions have not been used in the PLRF calculation because they are not reached in some of the cases and thus extrapolation would be required to calculate the PLRF.

PARAMETER STUDY RESULTS

Minor Road Figure 8 shows the increase in 95th percentile rutting as a function of cumulative load passes for cases 0, 1, 2 and 3 using $L_2 = 3.5$ in the subgrade rutting model. It can be seen from this figure that, for case 3, the pavement fails by excessive rutting after approximately 0.48 million vehicle passes. It can also be seen from this figure that, after the nominal failure condition has been passed, there is an increased rate of rutting. This is due to the non-linear relationship that exists between subgrade rutting and the thickness of the asphalt layer. From figure 8 it can be seen that the inclusion of surface roughness induced dynamic loads (case 1) and asphalt layer thickness variations (case 2) produce pavement life reductions PLRF of 48% and 58.7% respectively. Including both these effects (case 3) produce a PLRF of 66.7%. The SE values are 63.1% (case 0), 28.2% (case 1) and 16.5% (case 2).

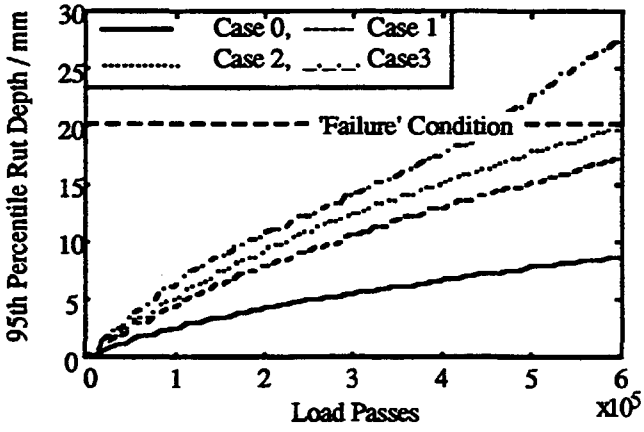

Figure 8. Accumulation of 95th percentile rutting on a minor road, using $L_2 = 3.5$.

Figures 9 and 10 show the increases in 95th percentile rutting and 95th percentile fatigue damage as a function of cumulative load passes for cases 0, 1, 2 and 3 using $L_2 = 1$ in the subgrade rutting model. It can be seen from these figures that, for case 3, instead of failing by rutting, the pavement lasts longer and fails by fatigue damage after approximately 0.55 million load passes. At failure, for case 3, the 95th percentile rut depth is only 1.5mm. This change in the mode of failure is due to the lower power in the subgrade rutting model reducing the weighting applied to the peaks of the dynamic loads and hence lowering the amplitude of the dynamic rutting damage in the subgrade. The SEs for cases 0, 1 and 2 are 90.6%, 69.4% and 70.9% respectively. PLRF values have not been calculated because the 95th percentile fatigue damage for case 0 does not reach 1. It can

be seen from this data that neglecting dynamic loads and asphalt layer thickness variations results in a 90.6% underprediction of the fatigue damage at failure.

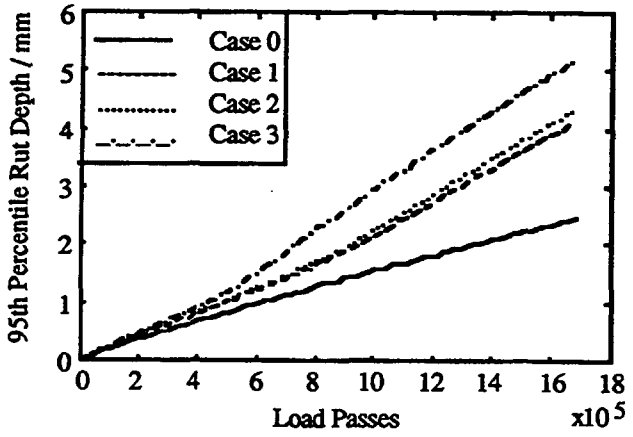

Figure 9. Accumulation of 95th percentile rutting on a minor road, using $L_2 = 1$.

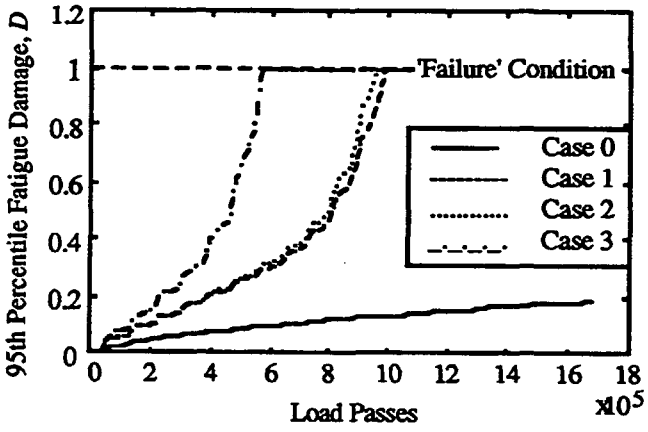

Figure 10. Accumulation of 95th percentile fatigue damage on a minor road, using $L_2 = 1$.

CONCLUSIONS

(1) A whole-life pavement performance model that is capable of making deterministic predictions of fatigue, rutting and surface roughness throughout the life of a pavement has been developed.

(2) The model includes the following features: (i) dynamic tyre forces, (ii) environmental effects, (iii) realistic pavement stiffness variations, (v) a realistic asphalt modulus degradation law due to fatigue damage, and (v) surface and subgrade rutting.

(3) Results from a preliminary case study indicate the considerable importance of the sensitivity in the subgrade rutting model on all aspects of flexible pavement wear (fatigue, rutting, roughness).

(4) Asphalt modulus degradation has been shown to have a significant effect on pavement wear, particularly when combined a large subgrade rutting exponent.

(6) For a thin pavement (125mm of asphalt), the failure mode was found to be dependent on the exponent in the subgrade rutting model. For a low power ($L_2 = 1$) the mode of failure was predicted to be fatigue, whereas for a high power ($L_2 = 3.5$) the mode of failure was predicted to be rutting.

(7) For a thin pavement (125mm) where the mode of failure was predicted to be fatigue, neglecting surface roughness induced dynamic loads and asphalt layer thickness variations results in a 90% underprediction of the fatigue damage at failure.

ACKNOWLEDGEMENTS

The authors are grateful to Mr George Ballard of GB Geotechnics Ltd for providing asphalt layer thickness data and Mr Nick Vertessy of ARRB for providing ALF deflection data.

REFERENCES

1. Collop, A.C. and Cebon, D., 'A model of whole-life flexible pavement performance.' IMechE J. Eng. Sci., (In Press).
2. Brademeyer, B.D., Delatte, N.J. and Markow, M.J., 'Analysis of moving dynamic loads on highway pavements. Part II: Pavement response.' Int. Symp. on Heavy Vehicle Weights and Dimensions, Kelowna, British Columbia, Canada, 1986.
3. Papagiannakis, A.T. *et. al.*, 'Impact of roughness-induced dynamic load on flexible pavement performance.' First. Int. Symp. on Surface Characteristics, Penn. State College, ASTM, 1988.
4. Ullidtz, P., 'Pavement analysis.' Developments in Civil Engineering, 19. Elsevier, 1987.
5. Ullidtz, P. and Stubstad, R.N., 'Modelling of pavement performance.' 7th Int. Conf. on Asphalt Pavements, Nottingham, UK, 1992.
6. Kujala, K., 'Frost action and the mechanical properties of an artificially frozen test plot.' 12th Int. Conf. on Soil Mechanics and Foundation Engineering, Rio de Janeiro, 1989.
7. Slunga, E. and Saarelainen, S., 'Determination of frost-susceptibility of soil.' 12th Int. Conf. on Soil Mechanics and Foundation Engineering, Rio de Janeiro, 1989.
8. Barber, E., 'Calculation of maximum pavement temperatures from weather reports.' Highway Research Board, Bulletin 168, 1957.
9. George, K.P. and Husain, S., 'Thickness design for flexible pavement: A probablistic approach.' Transp. Res. Rec. 1095 pp 27-36, 1986.
10. Robson, J.D., 'Road surface description and vehicle response.' Int. J. of Vehicle Design, 1 (1) pp 25–35, 1979.
11. Cebon, D. and Newland, D.E., 'The artificial generation of road surface topography by the inverse FFT method.' Proc. 8th IAVSD Symposium on the dynamics of vehicles on roads and on railway tracks, Cambridge, MA, 1984.
12. Sayers, M.W., Gillespie, T.D. and Paterson, W.D.O., 'Guidelines for conducting and calibrating road

roughness measurements.' World Bank, Technical Paper 46, 1986.
13. Cole, D.J., 'Measurement and analysis of dynamic tyre forces generated by lorries.' PhD Thesis, Cambridge University Engineering Department, 1990.
14. Cole, D.J. and Cebon, D., 'Validation of an articulated vehicle simulation.' Vehicle System Dynamics, 21 pp 197–223, 1992.
15. Cebon, D., 'Interaction between heavy vehicles and roads.' SAE SP–951, 930001, 1993.
16. Cole, D.J. and Cebon, D., 'Truck suspension design to minimise road damage.' IMechE J. Auto. Eng. (In Press).
17. Hardy, M.S.A., 'The response of flexible pavements to dynamic tyre forces.' PhD Thesis, Cambridge University Engineering Department, 1990.
18. Hardy, M.S.A. and Cebon, D., 'Importance of speed and frequency in flexible pavement response.' ASCE J. Eng. Mechs., 120 (3) pp 463–482, 1994.
19. Kenis, W.J., Sherwood, J.A. and McMahon, T.F., 'Verification and application of the VESYS structural subsystem.' Proc. 5th Int. Conf. on the Structural Design of Asphalt Pavements, 1 pp 333-345, 1982.
20. Gillespie, T.D. *et. al.*, 'Effects of heavy vehicle characteristics on pavement response and performance.' Transportation Research Board, NCHRP Report 353, 1993.
21. Yap, P., 'Truck tire types and road contact pressures.' 2nd Int. Symp. on Heavy Vehicle Weights and Dimensions, Kelowna, British Columbia, 1989.
22. Brown, S.F. and Brunton, J.M., 'An introduction to the analytical design of bituminous pavements (3rd edition).' University of Nottingham, Department of Civil Engineering, UK, 1992.
23. Anon, 'Residential course on bituminous pavements: materials, design and evaluation.' University of Nottingham, Department of Civil Engineering, 1992.
24. Brown, S.F., 'Material characteristics for analytical pavement design. Ch. 2.' In Developments in highway pavement engineering. Applied Science Publishers Ltd, London, 1978.
25. Powell, W.D. *et. al.*, 'The structural design of bituminous roads.' TRRL Laboratory Report LR 1132, 1984.
26. Anon, 'AASHTO guide for design of pavement structures.' American Association of State Highway and Transport Officials, Volume 1, 1986.
27. Bell, C.A. *et. al.*, 'Aging of asphalt-aggregate mixtures.' 7th Int. Conf. on Asphalt Pavements, Nottingham, UK, 1992.
28. Robertson, R.E. *et. al.*, 'Chemical properties and their relationships to pavement performance.' AAPT 60 pp 413-436, 1991.
29. Verhasselt, A.F. and Choquet, F.S., 'Comparing field and laboratory ageing of bitumens on a kinetic basis.' Presented at the 72nd Annual Meeting of the Transportation Research Board, Washington, DC, 1993.
30. Salter, R.J., 'Highway design and construction.' Macmillan Education, 1988.
31. Collop, A.C. and Cebon, D., 'A theoretical analysis of fatigue cracking in flexible pavements.' IMechE J. Eng. Sci, (In Press).
32. Chua, K.H., Der Kiureghian, A. and Monismith, C.L., 'Stochastic model for pavement design.' ASCE J. Transp. Engrg., 118 (6) pp 769-786, 1992.
33. Raad, L. and Marhamo, L.K., 'Evaluation of two-layer pavements using dimensional analysis.' Transp. Res. Rec. 1307 pp 99-110, 1992.
34. Cooper, K.E. and Pell, P.S., 'The effect of mix variables on the fatigue strength of bituminous materials.' TRRL, Laboratory Report 633, 1974.
35. Brown, S.F., Brunton, J.M. and Stock, A.F., 'The analytical design of bituminous pavements.' Proc. ICE, 79 pp 1-31, 1985.
36. Collop, A.C., Cebon, D. and Hardy, M.S.A., 'A visco-elastic approach to rutting in flexible pavements.' ASCE J. Transp. Eng., 121, No1 pp 1995.
37. Anon, 'A guide to the structural design of pavements for new roads.' RRL Road Note 29, 1970.
38. Brown, S.F. and Brunton, J.M., 'Improvements to pavement subgrade strain criterion.' ASCE J. Transp. Eng., 110 (6) pp 551-567, 1984.
39. Peattie, K.R., 'Flexible pavement design. Ch. 1.' In Developments in highway pavement engineering. Applied Science Publishers Ltd, London, 1978.
40. Croney, D., 'Is the measured deflection of a flexible pavement a reliable guide to life prediction and overlay design.' Highways Vol 58(Part 1986), 1990.
41. Kennedy, C.K., Fevre, P. and Clarke, C.S., 'Pavement deflection: Equipment for measurement in the United Kingdom.' TRRL Laboratory Report 834, 1978.
42. Wang, M.C. and Larson, T.D., 'Use of road rater deflections in pavement evaluation.' Transp. Res. Rec. 666 pp 129-150, 1978.
43. Johnson-Clark, J.R. *et. al.*, 'Data report on testing of full depth asphalt pavements: Mulgrave ALF trial.' ARRB, Research Report ARR No. 209, 1991.
44. Kadar, P., 'The performance of overlay treatments and modified binders under accelerated full-scale loading - The Callington ALF trial.' ARRB, Research Report ARR No. 198, 1991.
45. Collop, A.C., 'Effects of traffic and temperature on flexible pavement wear.' PhD Thesis, Cambridge University Engineering Department, 1994.
46. Maser, K.R. and Richter, C., 'Ground penetrating radar surveys to characterize pavement layer thickness variations at GPS sites.' Presented at Transportation Research Board 72nd Annual Meeting, Washington, DC, 1993.
47. Livneh, M. and Siddiqui, H.M., 'Assessment of radar technology for determining the thickness of pavement layers.' 7th Int. Conf. on Asphalt Pavements, Nottingham, UK, 1992.
48. Anon, 'National speed survey 1987.' Department of Transport, Statistics Bulletin (88)30, 1988.
49. Collop, A.C. *et. al.*, 'Investigation of spatial repeatability using a tire force measuring mat.' Transp. Res. Rec. 1448 pp 1-7, 1995.

50. Cole, D.J. *et. al.*, 'Spatial repeatability of measured dynamic tyre forces.' Submitted to IMechE J. Auto. Eng., 1994.

APPENDIX

This Appendix contains details of the WLPPM parameters used in the simulations.

SIMPLIFIED CASE STUDY

Pavement Property	Value
Maximum air temp. T_{air}^{max} /° C	10
Minimum air temperature T_{air}^{min} /° C	10
Asphalt layer thickness h_{asp} / mm	250
Percentage volume of bitumen V_b	12
Percentage volume of air voids V_v	4
Initial bitumen penetration $P^{(I)}$	50
Ageing constant Λ /° C^2 / hour	1.65×10^{-3}
Subgrade CBR percentage	4

PARAMETER STUDY

Speed Range, V m/s (Minor Road)	Suspension stiffness / MN/m
V≤13.4 (30mph)	0.396
13.4 (30mph)<V≤17.9 (40mph)	0.817
17.9 (40mph)<V≤22.4 (50mph)	1.616
22.4 (50mph)<V≤26.8 (60mph)	1.017

Pavement Property	Value
Maximum air temp. T_{air}^{max} /° C	18
Minimum air temperature T_{air}^{min} /° C	4
Asphalt layer thickness h_{asp} / mm	250
Percentage volume of bitumen V_b	12
Percentage volume of air voids V_v	4
Initial bitumen penetration $P^{(I)}$	50
Ageing constant Λ /° C^2 / hour	1.65×10^{-3}
Subgrade CBR percentage	4